

Phase Behavior of Polymer-Grafted Nanoparticles Blends Thin Film Induced by  
Solvent Annealing and Thermal Annealing

by  
Zihan Xiao

A thesis submitted to the Material Science and Engineering program, Cullen College  
of Engineering  
in partial fulfillment of the requirement for the degree of

Master of Science  
in Material Science and Engineering

Chair of Committee: Alamgir Karim  
Committee Member: Cunjiang Yu  
Committee Member: Devin L. Shaffer

University of Houston  
May 2020

## **Acknowledgments**

I am thankful and grateful to be guided by my advisor, Dr. Alamgir Karim, for helping me in these two years to have a deep sight of material science and engineering. His support and guidance are helpful and very much appreciated. Wenjie Wu also generously shared his expertise in the field.

I am grateful to all Karim research group members for their help and support throughout this journey. I am appreciative of the love and encouragement of my friends in the graduate school as well.

Finally, I want to thank my parents for their help in these two years. They raise me up when I feel upset and sluggish. Without their help and love I cannot finish my student career.

## Abstract

The grafting of polymer chains to nanoparticles has been found as an important method to control the particle assembly structures on a thin film state. We hypothesized that polymer-grafted nanoparticles blends have similar upper or lower critical solution temperature type phase behavior corresponding to linear polymer blends if the degree of polymerization is larger enough. UCST system we take is poly (methyl methacrylate) silica (PMMA-SiO<sub>2</sub>) and poly(styrene) silica (PS-SiO<sub>2</sub>), LCST system we take is PMMA-SiO<sub>2</sub> and poly(styrene)-(acrylonitrile) silica (PSAN-SiO<sub>2</sub>). Direct immersion annealing (DIA) method was used in switching the state of phase-separated structures in a binary blend film of UCST system, and thermal annealing method was used for the LCST system. Our results show that by varying the composition of the DIA solution, interchangeable phase separation state and homogeneous state are formed in the PMMA-SiO<sub>2</sub>/PS-SiO<sub>2</sub> blends thin film within 1 minute. The phase reversibility of UCST system is stable. Time-of-Flight Secondary Ion Mass Spectrometry (ToF-SIMS) reveals that the switchable phase separation state for UCST system occurs all throughout the film. However, for LCST system, phase reversibility is not feasible. We hypothesized a layered structure may formed underneath the surface of the thin film for this phenomenon. We believe that the phase reversibility of PGNPs blends will play an important role in the future nanoparticle-based material science and engineering.

## Table of Contents

Acknowledgments.....	ii
Abstract.....	iii
Table of contents .....	iv
List of Tables.....	v
List of Figures.....	vi
1. Introduction .....	1
2. Review of previous work.....	7
3. Experiment Results And Discussion .....	15
3.1 Phase reversibility of PS-SiO <sub>2</sub> /PMMA-SiO <sub>2</sub> system .....	15
3.1.1 As cast study of phase transition for PGNPs blends with ionic liquid ..	16
3.1.2 Time dependent study of PGNPs blends thin film with ionic liquid .....	17
3.1.3 Phase reversibility of PGNPs blends thin film with ionic liquid.....	20
3.1.4 Phase reversibility of PGNPs blends thin film .....	21
3.2 Phase behavior of other PGNPs blends brush system.....	27
3.2.1 As cast study of LCST system PGNPs brush with ionic liquid.....	28
3.2.2 Phase reversibility of PSAN-SiO <sub>2</sub> /PMMA-SiO <sub>2</sub> system .....	30
4. Conclusion .....	34
References.....	36

## **List of Tables**

Table 3.1 Summary of molecular characteristics of the particle brush system.....	15
Table 3.2 Summary of molecular characteristics of the particle brush system.....	28

## List of Figures

Figure 1.1 Schematic of a simple polymer-grafted nanoparticle.....	1
Figure 1.2 Schematic of PGNPs phase separation process.....	3
Figure 1.3 Schematic of athermal LCST blends.....	5
Figure 2.1 Morphology diagram from all of the date .....	8
Figure 2.2 SEM image of solvent mixture .....	9
Figure 2.3 DSC of PS and PMMA .....	10
Figure 2.4 Phase diagram of polymer .....	12
Figure 2.5 Reversible structure of PMMA-SiO <sub>2</sub> /PS-SiO <sub>2</sub> .....	13
Figure 3.1 Microstructure of [BMPPR][TFSI] .....	15
Figure 3.2 AFM image of as cast state transition progress for PGNPs .....	16
Figure 3.3 Time dependent study of PGNPs brush system .....	18
Figure 3.4 Schematic of phase reversibility of PGNPs .....	20
Figure 3.5 AFM phase images of PMMA-SiO <sub>2</sub> /PS-SiO <sub>2</sub> blends.....	22
Figure 3.6. ToF-SIMS in-depth profile for PMMA-SiO <sub>2</sub> /PS-SiO <sub>2</sub> blends.....	23
Figure 3.7 AFM phase separation images as a function of volume ratio of toluene in fixed ratio acetone.....	25
Figure 3.8 Schematic of PSAN-SiO <sub>2</sub> /PMMA-SiO <sub>2</sub> blends.....	29
Figure 3.9 Phase reversibility test for PSAN-SiO <sub>2</sub> /PMMA-SiO <sub>2</sub> blends.....	30
Figure 3.10 ToF-SIMS in-depth profile for PMMA-SiO <sub>2</sub> /PSAN-SiO <sub>2</sub> blends.....	32

# 1. Introduction

The remarkable and unique properties of nanocrystalline materials with limited size have been studied in past decades for applications in electronics,<sup>1</sup> sustainable energy and magnetic storage.<sup>2-3</sup> Looking through the long river of history, the earliest research on polymer nanocrystalline came from Bakelite's attempt in the 1900s to strengthen wood through impregnation of resin.<sup>4</sup> A wide applications of polymer nanocrystalline was discovered and innovated after that age.

The polymer-grafted nanoparticle is one of the most popular research fields in polymer nanocrystalline. Properties of polymer grafted nanoparticles were shown to sensitively depend on the grafting density and the degree of polymerization of the grafted chains.<sup>5</sup> Figure 1.1 shows a simple schematic of polymer grafted nanoparticles,

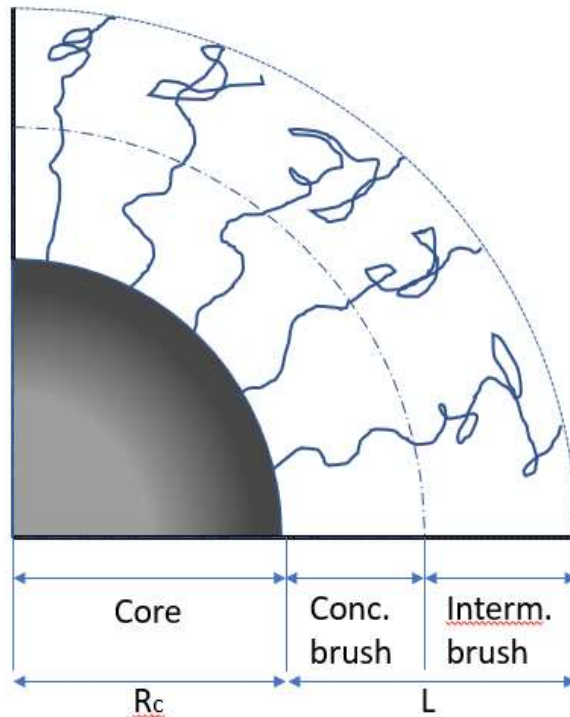


Fig 1.1 Schematic of a simple polymer-grafted nanoparticle where  $R_c$  is the radius of the nanoparticle's core,  $L$  is the length of the polymer brush.

There are two parts of the polymer brush region: (1) the concentrated brush regime, which is characterized by high grafting density  $\sigma$ ; (2) the intermediate brush regime, which is characterized by a reduced grafting density and relaxed polymer conformation.<sup>6</sup> Based on the nature of polymer-grafted nanoparticles(PGNPs), the grafting density of polymer which is also the degree of polymerization  $N$  will have an obviously impacts on the phase behavior of PGNPs blends.

The phase behavior of polymer blends is largely governed by the Flory-Huggins interaction parameter  $\chi$ . The Flory-Huggins equation<sup>7</sup> is given below,

$$\frac{\Delta G_m}{k_B T} = \frac{\phi_1}{N_1} \ln \phi_1 + \frac{\phi_2}{N_2} \ln \phi_2 + \chi \phi_1 \phi_2 , \quad \text{Equation 1.1}$$

where  $\Delta G_m$  is the mixing free energy of polymer blends,  $k_B$  is the Boltzmann constant,  $T$  is the temperature,  $\phi_1$  and  $\phi_2$  are the volume fraction of two different polymers,  $N$  is the degree of polymerization,  $\chi$  is the interaction parameter which is also the Flory-Huggins interaction parameter. The mixing free energy of polymer can be affected by entropic contribution and enthalpic contribution. As is shown in Equation 1.1,  $\frac{\phi_1}{N_1} \ln \phi_1 + \frac{\phi_2}{N_2} \ln \phi_2$  is contributed to the entropic contribution,  $\chi \phi_1 \phi_2$  is contributed to the enthalpic contribution.<sup>8</sup>  $\chi$  can be also written as below,

$$\chi = a + \frac{b}{T} , \quad \text{Equation 1.2}$$

where  $a$  stand for the entropic part and  $b$  stands for the enthalpic part. As is shown in Equation 1.2, the Flory-Huggins parameter is a temperature dependence parameter. Based on Tombasco's research,<sup>9</sup> when  $\chi$  is positive, there will be an upper critical solution temperature (UCST) for polymer blends phase behavior. On the contrary, when  $\chi$  is negative, there would be a lower critical solution temperature (LCST). Therefore,



for thermal annealing conditions, cooling or heating polymer brush would lead to the phase transition.

Polymer-grafted nanoparticles blends have a similar phase behavior as polymer blends. In figure 1.2, it illustrates the process that the phase transition of PGNPs blends when the temperature changes.

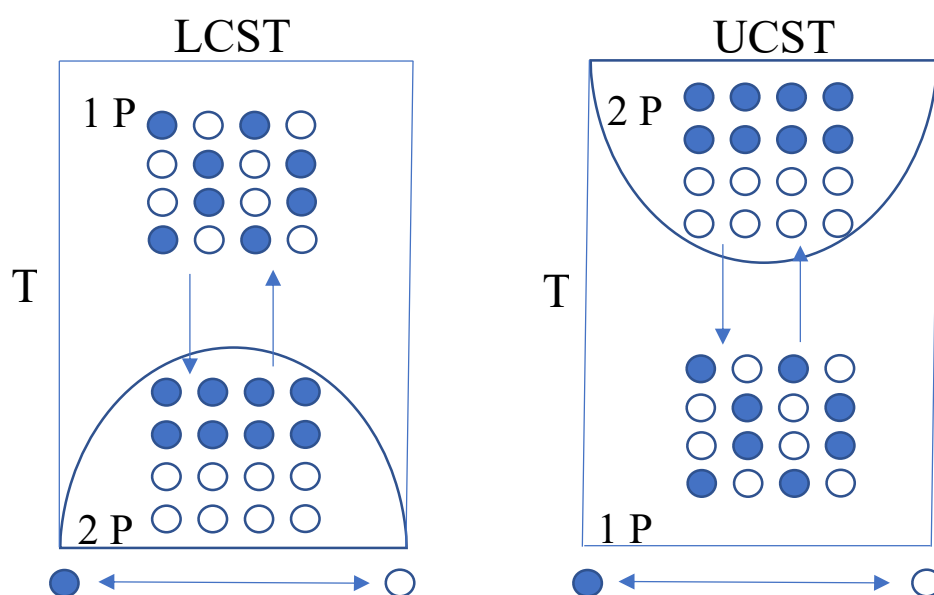


Figure 1.2 Process of polymer grafted nanoparticles blends' phase separation

One phase in polymer-grafted nanoparticles blends is for the homogeneous state, and two phases region for polymer-grafted nanoparticles blends is for phase-separated state. As is shown in Figure 1.2, there is a critical temperature for both LCST system and UCST system, which is also known as the cloudy point. Flory-Huggins parameter  $\chi$  can be different from the temperature difference. Thermal annealing can make both LCST and UCST system's phase transit from homogeneous state to phase separation state.

Besides thermal annealing conditions, solvent annealing can also make phase separation of PGNPs blends happen. Solvent annealing, which is also called direct

immersion annealing (DIA), has been found that can make phase separation of thin block copolymer thin film.<sup>10</sup> Compared to thermal annealing, direct immersion annealing can take the glass transition temperature ( $T_g$ ) to the room temperature ( $R_t$ ), and it is much faster than TA when achieving phase separation. There are two important factors of direct immersion annealing: the first one is the solvent mixture needs to be selected carefully. A poor or marginal solvent with a good solvent mixture will be chosen for block copolymer systems in order to achieve a well-ordered morphology.<sup>11</sup> The function of a poor solvent in the mixture is to control the rate of polymer film dissolution. Secondly, the ratio of the good solvent in a solvent mixture (SM) needs to be considered carefully. For example, for the PS-PMMA block copolymer system, heptane is a nonsolvent for both PS and PMMA, acetone is a good solvent for PMMA but a marginal solvent for PS. Usually, a ratio of acetone to heptane is 1:2. However, if the ratio of acetone becomes much larger, a thin block copolymer film could be washed out. Typically, a selective solvent would make polymer blends thin film phase separation, a neutral solvent would achieve a homogeneous state. A schematic of the DIA process is shown in Figure 1.3,

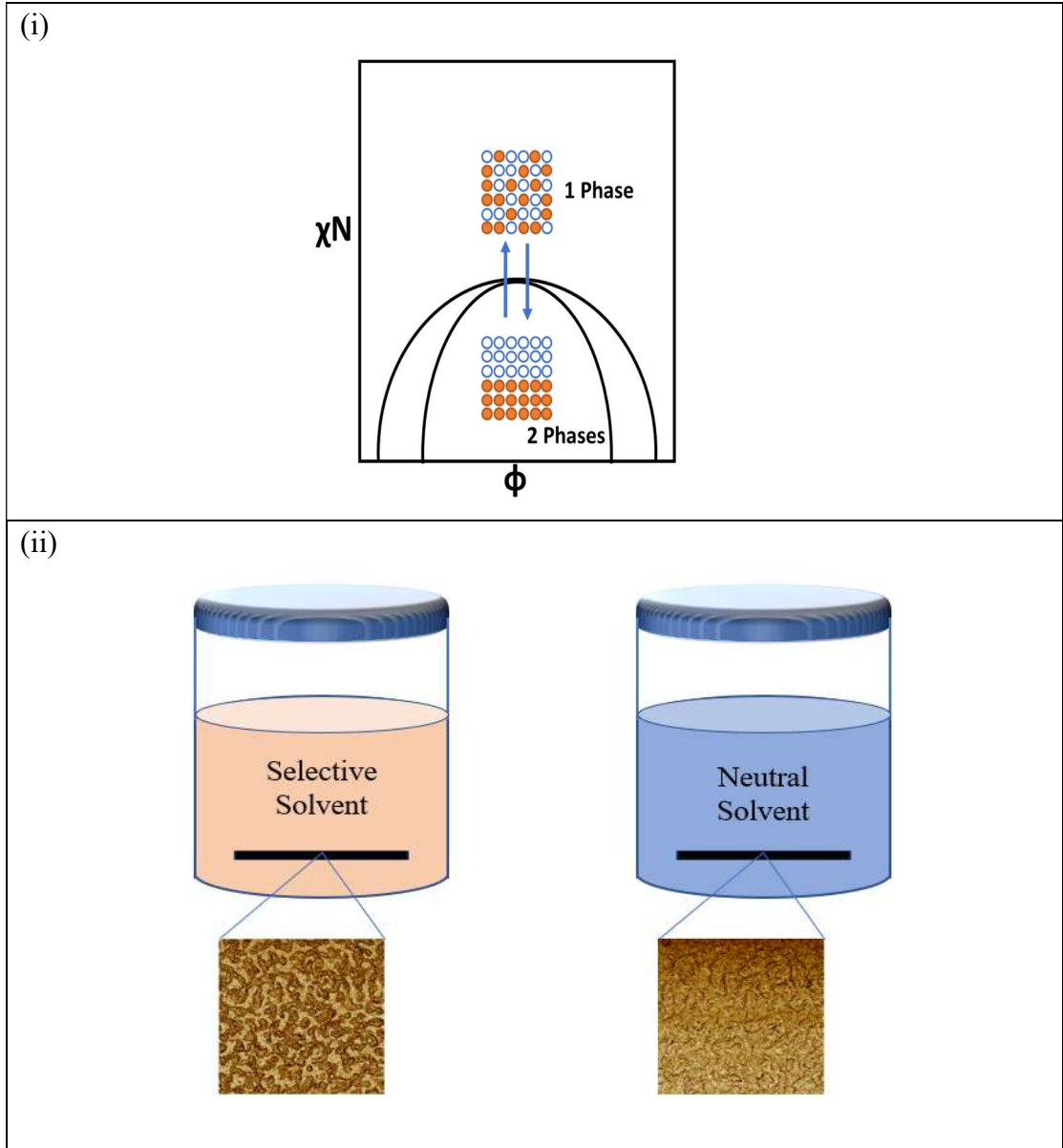


Figure 1.3 (i) Schematic of proposed reversible phase separation of athermal LCST blends. (ii) Schematic of reversible phase separation of PGNP blends using DIA

figure (i) in Figure 1.3 shows that there is a critical  $\chi N$  point for the UCST system's phase transition. Typically, the critical  $\chi N$  point for block copolymers system is 10.5, but for polymer blends system is around 2.<sup>12</sup> The Flory-Huggins parameter  $\chi$  in DIA system would be affected by two different polymer-solvent interaction parameters, which can be expressed as the following equation:

$$\chi_{12} = \frac{(\chi_{1s} - \chi_{2s})^2}{(\delta_1 + \delta_2 - 2\delta_s)^2} \frac{RT}{v}, \quad \text{Equation 1.3}$$

where  $\chi_{ij}$  represents the Flory-Huggins interaction parameter between component  $i$  and  $j$ ,  $\delta$  is the Hansen solubility parameter, and 1,2 represents polymers while  $s$  indicates the solution.<sup>13</sup> For PGNPs blends in DIA system, the phase separation will depend on the polymer grafting density (degree of polymerization) and the polymer-solvent interaction parameter.

In this work, we are managed to make a reversible phase separation between two different systems: UCST system: PS-SiO<sub>2</sub> and PMMA-SiO<sub>2</sub> and LCST system: PSAN-SiO<sub>2</sub> and PMMA-SiO<sub>2</sub>. We also tried to use ionic liquid as an additive to check its impacts on the phase separation of polymer-grafted nanoparticles. Results and details will be discussed in Chapter 3 and Chapter 4.

## 2. Review of previous work

In this paper, there are three main part will be discussed: 1. The impact of ion liquid on the phase separation of PS-SiO<sub>2</sub> and PMMA-SiO<sub>2</sub> blends thin film; 2. Deep research of the phase reversibility of PS-SiO<sub>2</sub> and PMMA-SiO<sub>2</sub> blends thin film; 3. Additional research on the phase reversibility of PSAN-SiO<sub>2</sub> and PMMA-SiO<sub>2</sub> blends thin film.

For phase separation of PGNPs blends, the properties of PGNPs are researched firstly. Choi and his coworkers indicated that by changing the grafting density of polymer-grafted nanoparticles (PGNPs), the system properties can be altered between 'hard-sphere like' and 'star polymer-like' behaviors.<sup>14</sup> Through their later research, they found that the PGNPs can form polymer-like crazing with enhanced elastic and mechanical properties when the outer brush is in the semi-dilute polymer brush (SDPB) region.<sup>15</sup> This kind of property of PGNPs can be used in making hybrid material. Nevertheless, for some applications, a sub-micron domain with a well-controlled manner need to be achieved. This needs us to research the phase dispersion or the separation of PGNPs blends. Kumar revealed that the phase separation behavior depends on the grafting density of PGNPs ( $\sigma$ ) and the degree of polymerization of both polymer matrix (P) and PGNPs (N). As is shown in Figure 2.1, where  $\alpha$  equals to N/ P, they found out that with the higher grafting density PGNPs, which is also a larger size of PGNPs, the blends will reside in either phase separation (PS) or good dispersion (WD) state. However, with the lower grafted PGNPs, it will form into a range of structures, including strings (S), connected sheets (CS), and small clusters (SC), which is likely caused by the core-core attractions and brush physics.<sup>16-17</sup>

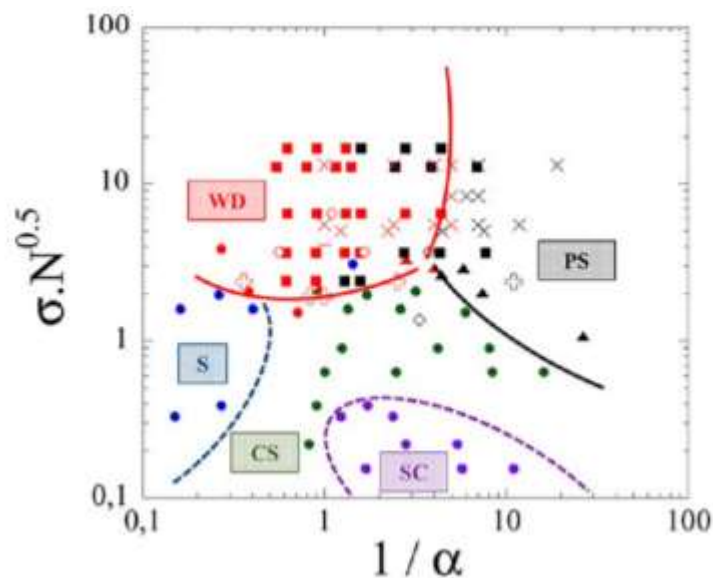


Fig 2.1 A composite morphology diagram created from the available data in the literature:  $\sigma\sqrt{N}$  as a function of  $1/\alpha$  with  $\alpha = N/P$ .<sup>16-17</sup>

As is shown in figure 2.1, the red point corresponds to well dispersed particles (WD); black to phase separated samples (PS); blue to strings (S); green to connected sheets (CS) and purple to small clusters (SC).<sup>16-17</sup> Karim's group reveals that the chemistry of the inner organic core can also influence the dispersion of PGNPs.<sup>18</sup> All of these researches are focused on the properties of PGNPs blends. But for the phase separation of PGNPs blends, it has just been found out recently. Based on Bockstaller's research, he has revealed that ligand interactions between the two PGNPs can drive it into phase separation state like homopolymer mixtures. By conducting thermal annealing on different kinds of PGNPs mixtures, they revealed that PGNP blends can show the same LCST/UCST behavior like the corresponded homopolymer mixtures.<sup>19</sup>

On the other hand, some researchers have found that ionic liquid can make a significant impact on the phase separation process of a block copolymer. According to Nealey's group work, introduce ionic liquid(IL) such as N-butyl-N-

methylpyrrolidiniumbis-(trifluoromethylsulfonyl)imide ([BMPR][TFSI]) to PS-b-PMMA system allows that ionic liquid to be incorporated only into the polar PMMA block.<sup>20</sup> The result is shown in Figure 2.2.

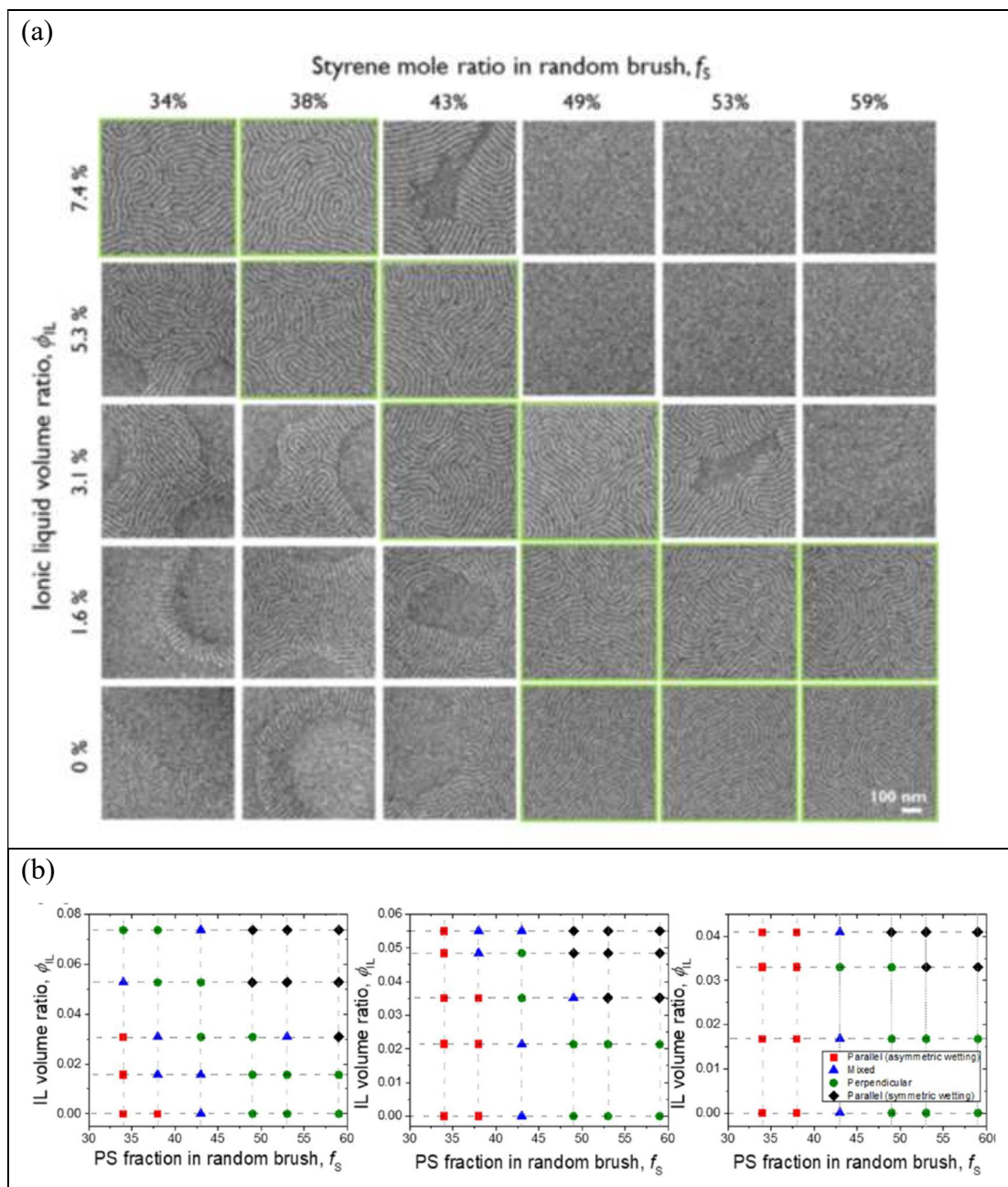


Fig 2.2 (a) Top-Down SEM image of solvent mixture. P(S-r-MMA) depends on different ionic liquid volume ratio and styrene ratio; (b) Maps of the orientation of self-assembled PS-b-PMMA in thin films when blended with different ionic liquid from left to right.<sup>20</sup>

As is shown in (a) in Figure 2.2, for the same polystyrene component for example 49% styrene mole ratio in the random brush, with the increase of the volume ratio of ionic liquid, the perpendicular orientations of the random brush surface become faded away. This phenomenon means that the ionic liquid can increase the effective interaction parameter ( $\chi_{\text{eff}}$ ) and a higher ratio of ionic liquid in the PS-b-PMMA brush system requires less styrene to maintain the perpendicular orientations. Besides the impact of ionic liquid on the interaction parameter of PS-b-PMMA brush system, it can also affect the glass transition temperature ( $T_g$ ) of these two homopolymers. The changing of  $T_g$  is shown in figure 2.3.

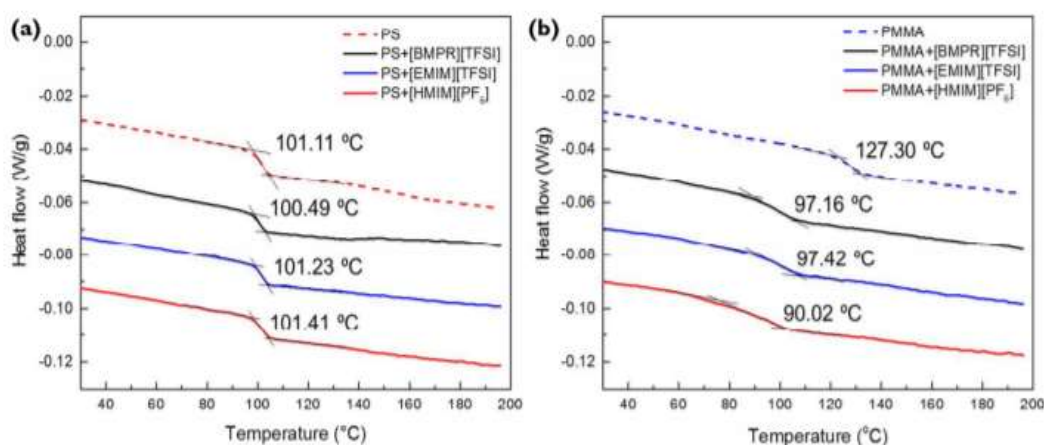


Figure 2.3 Differential Scanning Calorimetry (DSC) scans of a) PS and b) PMMA before and after blending with ionic liquid (20 wt%) of [BMPR][TFSI], [EMIM][TFSI] and [HMIM][PF<sub>6</sub>] respectively. Scans are offset vertically for clarity<sup>20</sup>

As is shown figure 2.3, the glass transition temperature ( $T_g$ ) of the PMMA homopolymer decreased by 30.1, 29.9, and 37.3 °C after being mixed with 20 wt % different types of ionic liquid, respectively. Nonetheless, there is no significant changes in the  $T_g$  were measured in the PS homopolymer upon the addition of ionic liquid.<sup>20</sup> The lack of plasticization in the PS homopolymer, therefore, indicates that a



homogeneous blend of the PS and ionic liquid is not formed. This selective compatibility allows the ionic liquid to be incorporated only into the polar PMMA block when added to the PS and PMMA homopolymer blends, thus enhancing the segregation strength between the two blocks as described by the effective interaction parameter ( $\chi_{\text{eff}}$ ) owing to the unfavorable interaction between PS and ionic liquid.<sup>29-31</sup>

Based on the previous study of the properties of PGNPs blends and the impact of ionic liquid on the self-assembly of a block copolymer, in our work, we tried to investigate the phase reversibility of polystyrene-silica(PS-SiO<sub>2</sub>) and poly(methyl methacrylate)-silica(PMMA-SiO<sub>2</sub>) and the effect of ionic liquid on the phase separation of PGNPs blends. This blend is called the athermal system, where the Flory-Huggins interaction parameter doesn't vary a lot, which makes it impossible to achieve reversible and controllable phase separation thermally. We developed a solvent assisted annealing method named direct immersion annealing (DIA) to help control the morphologies of PGNP blends. DIA was recently developed and has been applied in the study of block copolymer phase separation.<sup>21-23</sup> Different from the traditional solvent vapor annealing (SVA), it directly put the polymer films into the solvent mixture. The solvent mixture contains the selective solvent to one of the blocks and can help induce the phase separation. Non-solvent for both blocks is also added to avoid the dissolution of polymers into the solution. To our knowledge, this is the first research on PGNP blends using direct immersion annealing. We believe the better and reversible control of the PGNP blends can provide a better application of PGNPs.

For another system, poly(styrene-acrylonitrile)-silica(PSAN-SiO<sub>2</sub>) and PMMA-SiO<sub>2</sub>, there are few works about this system. According to Noboro's work, they found out that the interaction parameter  $\chi$  of SAN/PMMA system would decrease with the temperature increasing. The temperature dependence can be considered as a linear relationship of  $\chi$  versus the reciprocal temperature ranging from 140°C to 170°C. Zhou's group<sup>25</sup> has found out that the critical phase separation point which is also the cloud point of SAN and PMMA homopolymer blends. It has been found that the cloud point will be changed ranging from 155°C to 160°C by changing the ratio of SAN and nanoparticles as is shown in Fig 2.3.

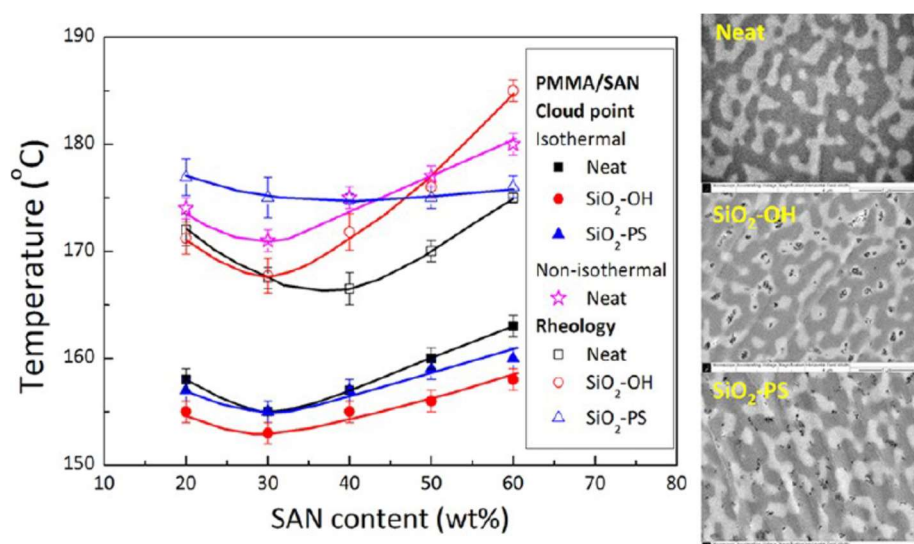


Figure 2.4 Phase diagram of PMMA/SAN, PMMA/SAN/SiO<sub>2</sub>-OH, and PMMA/SAN/SiO<sub>2</sub>-PS blends.

PSAN and PMMA will present a phase separation state when they are homopolymer blends. Paul and his co-workers found that the PSAN and PMMA copolymer blends is an LCST system which means that upon this system's cloudy point it will present a phase separation state and below the cloudy point it will show a homogeneous state. It shows a reversible transition between miscible and phase-separated states provided that

the molar ratio  $N_{AN}/N_S$  is within the miscibility window 0.09~0.38.<sup>25</sup> The interaction parameter of the PSAN/PMMA homopolymer brush system depends on both the constitution of PSAN as well as the composition of the blend. In our work, the molar composition of the PSAN is S/AN = 3: 1, and the corresponding interaction parameter is PMMA/SAN  $\approx -0.15$  (at  $T \approx 25^\circ\text{C}$ ). As is state before, the polymer blends system will present an LCST behavior when the interaction parameter is below zero. The LCST of linear PMMA / PSAN blends is approximately 160  $^\circ\text{C}$  for a polymer molecular weight of is around 90,000.<sup>26-27</sup> Then based on Schmitt's work, the PSAN-SiO<sub>2</sub> and PMMA-SiO<sub>2</sub> PGNPs blends in a thin film state will present phase reversibility as is shown Figure 2.4,

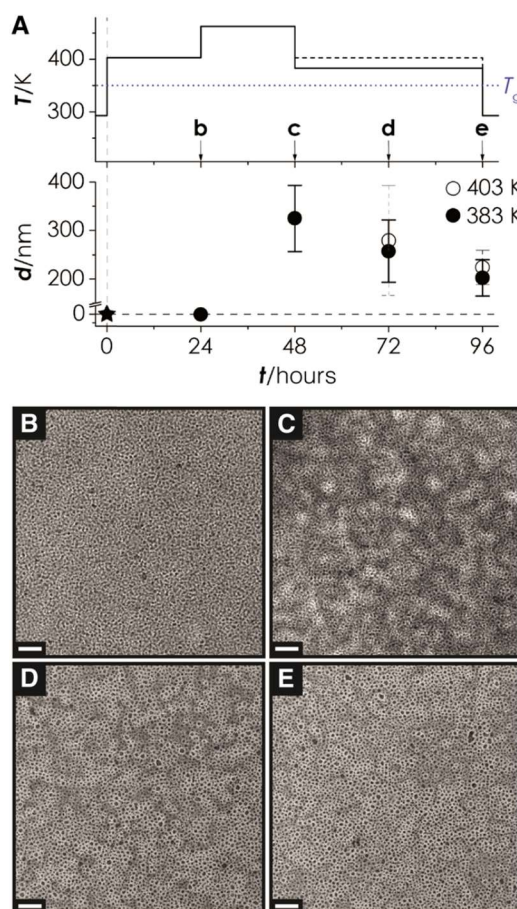


Figure 2.5 Reversible structure evolution in SiO<sub>2</sub>-MMA257/SiO<sub>2</sub>-SAN262 (50:50) LCST system<sup>26-27</sup>

the cloudy point is around 160°C which correlates well with the expected behavior of linear PMMA/PSAN blends.<sup>28</sup> In their work, the degree of polymerization and the molecular weight of PSAN-SiO<sub>2</sub> and PMMA-SiO<sub>2</sub> are almost the same. In that case, the interaction parameter of these two polymer-grafted nanoparticles will be well controlled.

In our work, we focus on developing the phase reversibility of two different systems: UCST system-PS-SiO<sub>2</sub>(R<sub>c</sub>=55 nm) and PMMA-SiO<sub>2</sub>(R<sub>c</sub>=59 nm) and LCST system-PSAN-SiO<sub>2</sub>(R<sub>c</sub>=30 nm) and PMMA-SiO<sub>2</sub>(R<sub>c</sub>=36 nm). The phase separation method we used is thermal annealing and direct immersion annealing. Ionic liquid is used as the additive to see its impacts on the phase separation of these two systems. Results will be discussed in the next two chapters.

### 3. Experiment Results And Discussion

#### 3.1 Phase reversibility of PS-SiO<sub>2</sub>/PMMA-SiO<sub>2</sub> system

In the chapter, we are going to show the result of phase reversibility of the UCST system: PS-SiO<sub>2</sub> and PMMA-SiO<sub>2</sub>. First, we tried to add several sets of ionic liquid to the PGNPs blends to see its impact on the phase separation. Ionic liquid we used for this experiment is N-butyl-N-methylpyrrolidinium-bis(trifluoromethylsulfonyl)imide ([BMPR][TFSI]). The microstructure of this ionic liquid is shown in Figure 3.1,

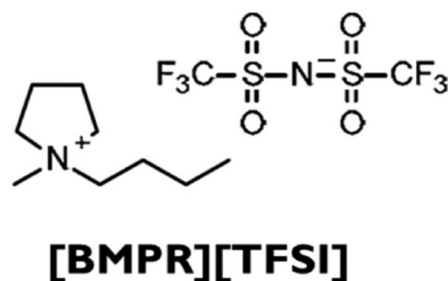


Figure 3.1 Microstructure of [BMPR][TFSI]

the properties for the PGNPs brush system are shown as the Table 3.1 below:

Table 3.1 Summary of molecular characteristics of particle brush system

Sample	N	Mn	Rc/nm	$\sigma/\text{nm}^{-2}$
PS-SiO <sub>2</sub>	35000	336	55	0.52
PMMA-SiO <sub>2</sub>	32500	320	59	0.56

we also measured the surface roughness transition trend for PGNPs brush system with different ratios of the ionic liquid. A comparison between the polymer-grafted nanoparticles brush system with or without ionic liquid is being discussed. A time dependent study for PGNPs brush system was also studied. Finally, the phase reversibility of PGNPs brush system was investigated and successfully developed for thin films without adding ionic liquid. The experimental instrument used in this chapter including AFM and ToF-Sims. The annealing method used in this experiment is the

direct immersion annealing.

### 3.1.1 As cast study of phase transition for PGNPs blends with ionic liquid

In this experiment, the PGNPs volume ratio is PS-SiO<sub>2</sub>: PMMA-SiO<sub>2</sub>=50:50. The ratio of ionic liquid selected for this experiment is 0%, 1%, 5%, 10%, 25%, which is respected to the volume of PMMA-SiO<sub>2</sub>. Thickness of thin films is around 100 nm. The as-cast state transition trend of PGNPs blends thin films,

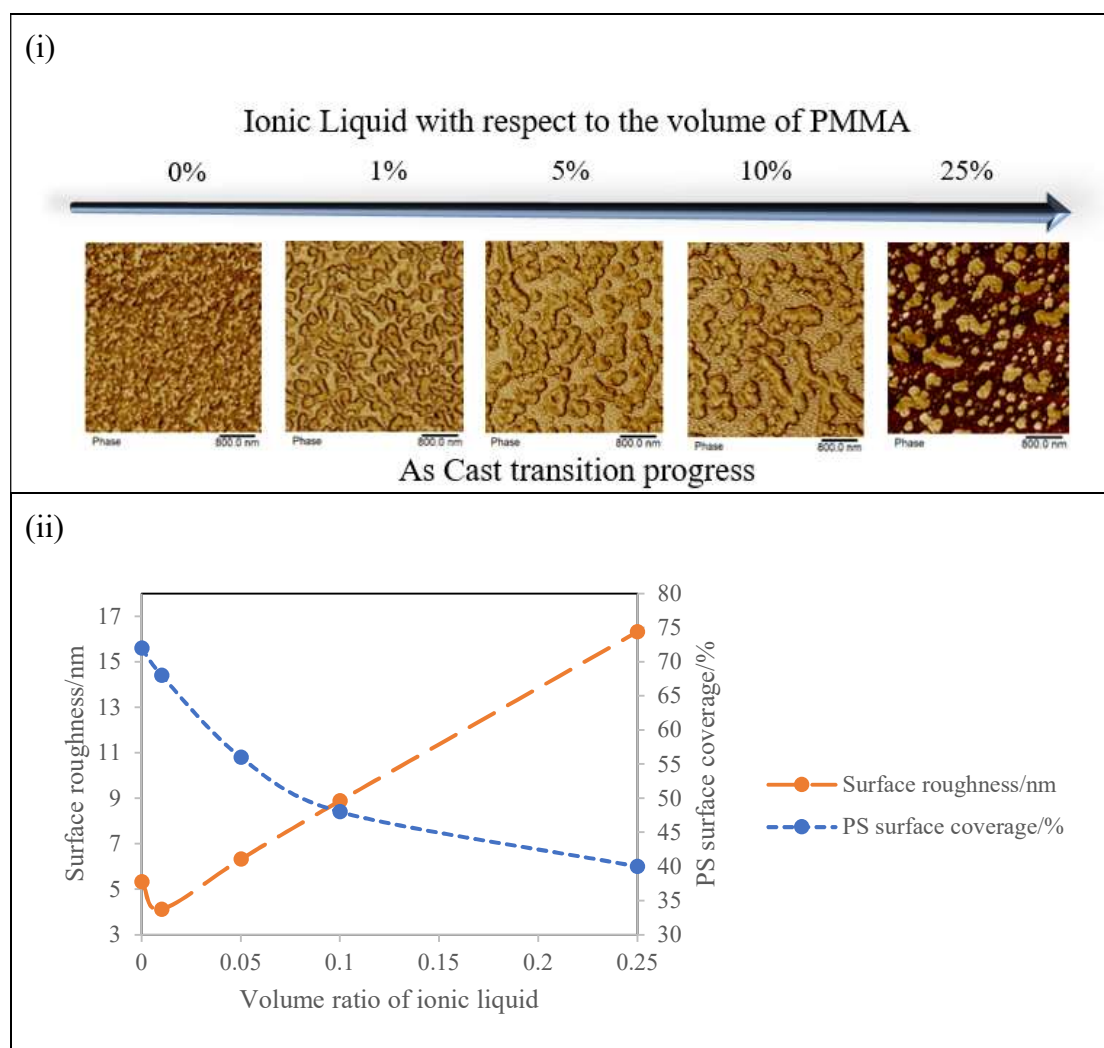


Fig 3.2 (a)AFM image of as-cast state transition progress for PGNPs blends thin films with different ionic liquid ratio; (b) Surface roughness changing trend for PGNPs blends thin film with different ionic liquid ratio.

the dark region in phase images (a) is the PS domain, and the light area is the PMMA domain. For film with 25% ionic liquid, the dark region is the PMMA domain, and the

light area is the PMMA domain. As is shown in figure 3.2 (a), with increasing the volume ratio of ionic liquid, the self-assembly of each polymer-grafted nanoparticle becomes more apparent even for adding 1% to the PGNPs blends. As is stated before, the interaction parameter  $\chi$  will increase when ionic liquid is added to the PGNPs brush system. But the phase separation state is determined by  $\chi N$  as is shown in figure 1.3. The Flory-Huggins interaction parameter for PS/PMMA is  $\chi_{S/MMA} = 0.028 + 3.9/T$ , where T is the absolute temperature.<sup>29</sup> The critical point of  $\chi N$  for polymer blends is around 2 when the weight ratio of two polymers is 50:50. Even a small change of the interaction parameter will not interact with the phase separation state of PGNPs brush since the molecular weight is the same. Figure 3.2 (b) present the surface roughness transition of PGNPs brush system with different ratio of ionic liquid. With increasing the ratio of ionic liquid, the surface would become rougher.

### **3.1.2 Time dependent study of PGNPs blends thin film with ionic liquid**

Except the as cast study of PGNPs brush with different ratios of ionic liquid, we also tried the time dependent study of using DIA method to show the phase transition progress. We take ace:hep=1:1 as the selective solvent to see the phase transition. While heptane is a nonsolvent for both PS and PMMA, acetone is a good solvent for PMMA and a marginal solvent for PS. Hence, acetone only plasticizes the PS block to a limited extent, but sufficiently for enhancing overall block copolymer mobility.<sup>32-33</sup> We believe the same DIA solution composition can be applied to the PGNPs blends thin film. The selective solvent selected in this experiment acetone and heptane which ratio is 1:2. The neutral solvent selected for this experiment is toluene and heptane which ratio is 1:2.

The time dependent study for different ionic liquid ratio on the phase separation of PGNPs brush system result is shown as in Figure 3.3,

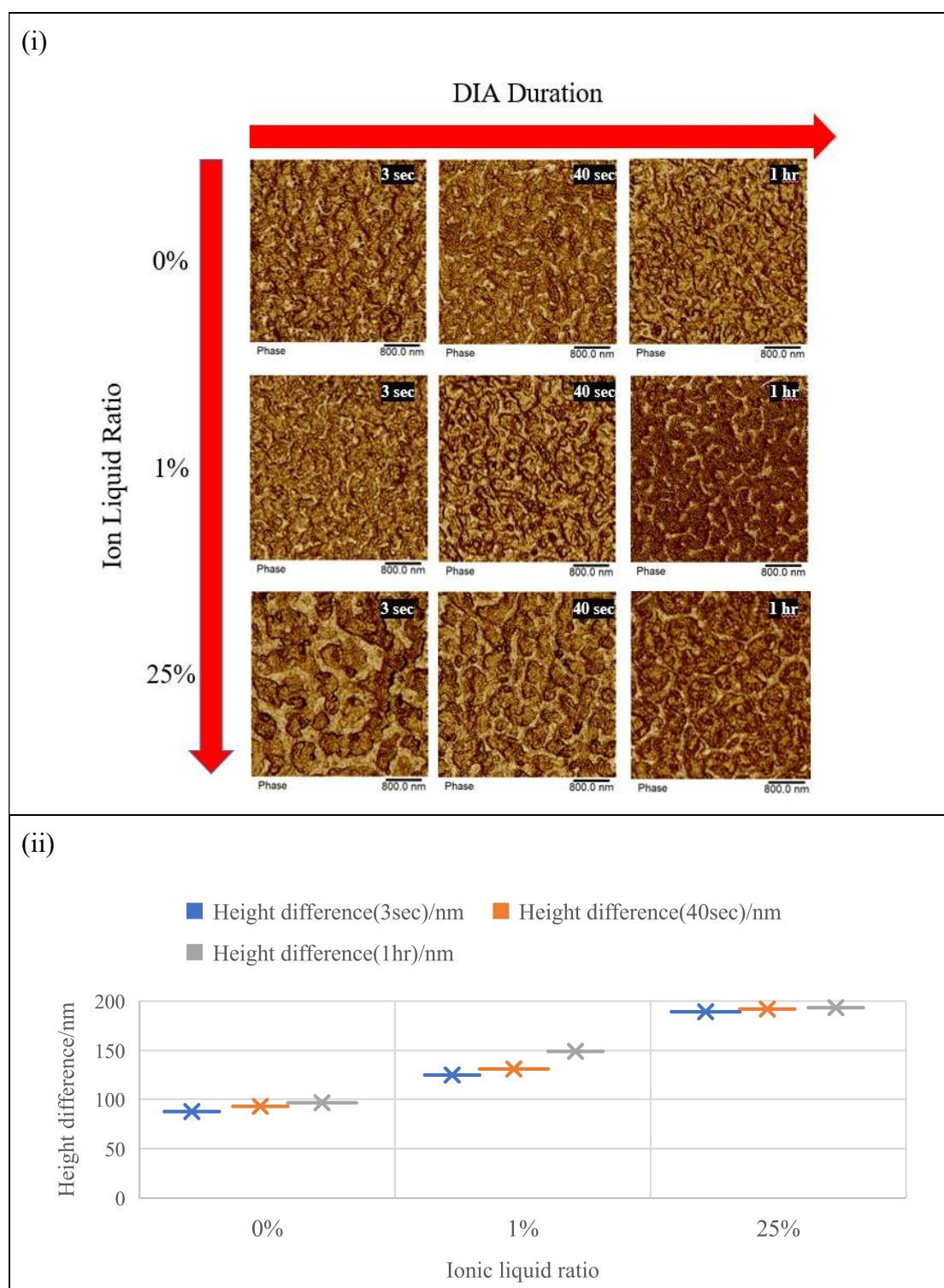


Figure 3.3 (i) Time dependent study of PGNPs brush system with different ratio of ionic liquid phase transition progress in a selective DIA solution; (ii) Height difference image of PGNPs blends thin film with different ionic liquid ratio



since ionic liquid will increase the Flory-Huggins interaction parameter of PGNPs brush, putting PGNPs blends thin film into a selective solvent for several minutes should make a trend back to the two phases state. Figure 3.3 (i) shows that for PGNPs brush with 0% ionic liquid, DIA will not make a significant difference on the surface phase separation state. However, for PGNPs brush thin films with ionic liquid, a selective solvent will make a domain size change of two different PGNPs, especially for PGNPs brush with 25% ionic liquid. In figure 3.3, white block stands for PMMA-SiO<sub>2</sub>, where dark block stands for PS-SiO<sub>2</sub>. With thin films annealed in a selective solvent, two blocks' domain area was inversed. This is because of that unfavorable interaction between PS and acetone. PS-SiO<sub>2</sub> will squeeze to the bottom of the PGNPs blend thin film since this kind of unfavorable interaction. For PGNPs blends thin film with 0% ionic liquid annealed for 40 sec, it presented a similar structure with PGNPs blends thin film with 1% ionic liquid annealed for 3 sec. The reason for this phenomenon is because of adding ionic liquid into this PGNPs blends brush system will increase the Flory-Huggins interaction parameter  $\chi$  and accelerate the phase separation behavior. This PGNPs blends thin film could present a desired phase separation state with less time when adding a small amount of ionic liquid.

In figure 3.3 (ii), a calculated height difference image was presented. Increasing the ionic liquid ratio could induce a big difference of height. We designed a phase reversibility experiment for PGNPs blends thin film with ionic liquid to see the impact of ionic liquid on the phase reversibility.

### 3.1.3 Phase reversibility of PGNPs blends thin film with ionic liquid

Based on the conclusion that ionic liquid will affect the phase separation progress of PGNPs blends. We also tried the phase reversibility test of PGNPs blends thin films with ionic liquid. PGNPs blends thin films are immersed in a selective solvent (Acetone: heptane=1:1) and neutral solvent (toluene: heptane=1:1) for 3 minutes to see the phase reversibility. Figure 3.4 shows the result,

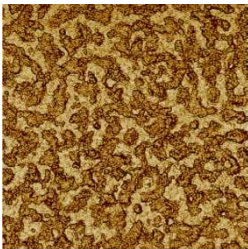

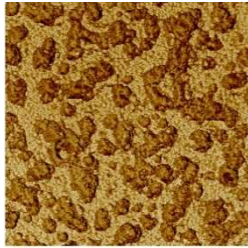

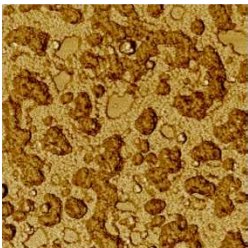
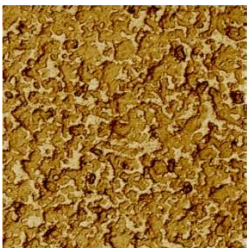
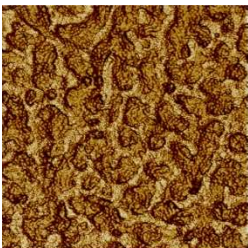
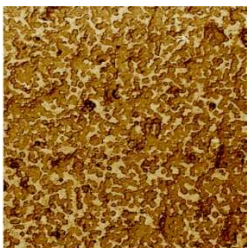
Ionic liquid ratio	Selective solvent	Neutral solvent
1%		
5%		
10%		
25%		

Figure 3.4 Schematic of phase reversibility of PGNPs blends thin films with different ionic liquid ratio

in figure 3.4, from a) to b, a) shows the phase separation state, b) presents a homogeneous state, thus it is obvious to see the phase reversibility. However, with increasing the ionic liquid ratio, the phase reversibility is not clear. From c) to d), c) stay in a phase separation state, but d) presents a semi-homogeneous state of its surface. This phenomenon is much more notable for PGNNPs blends with 10% and 25% ionic liquid. Even though e) and g) show a phase separation state, f) and h) still stays in a phase separation state. As is clarified before, adding ionic liquid to the PGNNPs blends will increase the Flory-Huggins interaction parameter  $\chi$  and change the phase surface roughness. For PGNNPs blends with much more ionic liquid, the Flory-Huggins interaction parameter  $\chi$  will be changed a lot and the phase reversibility will be destroyed. Therefore, based on figure 3.4, when the volume ratio of ionic liquid is more than 5% respected to the volume of PMMA-SiO<sub>2</sub>, the phase reversibility will fade away. In order to circumvent this kind of situation, we managed to do a phase reversibility experiment for PGNNPs brush system without ionic liquid.

#### **3.1.4 Phase reversibility of PGNNPs blends thin film**

In this chapter, we tried to use AFM to show the phase reversibility of PGNNPs blends without ionic liquid. PGNNPs blends thin films are immersed in a selective solvent and neutral solvent to induce the phase behavior for 3 minutes. Figure 3.5 shows the result,

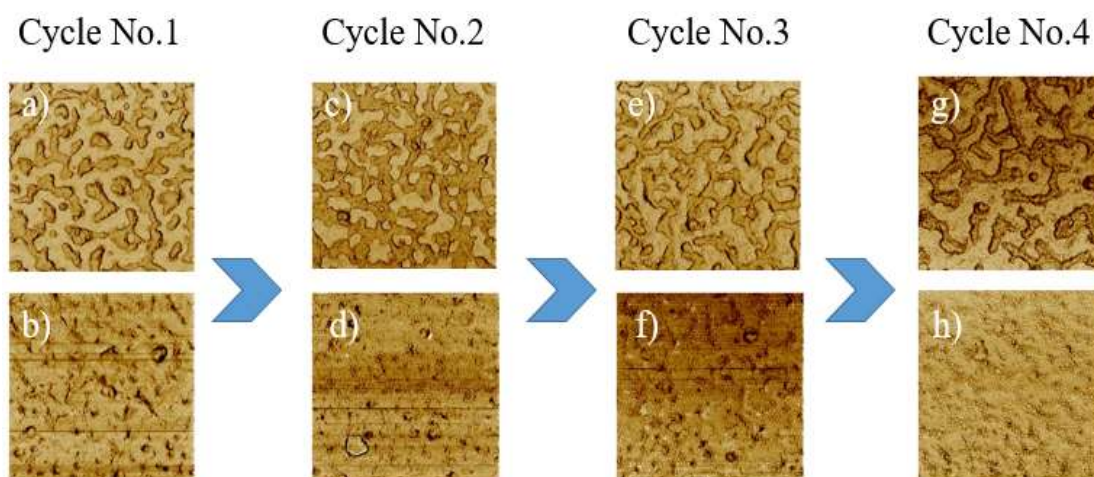


Figure 3.5 AFM phase images of PMMA-SiO<sub>2</sub>/PS-SiO<sub>2</sub> blends indicating highly reversible phase separation by using two different DIA solutions. Scale bar:800nm

figure 3.5 (a) is a phase image of a certain PMMA-SiO<sub>2</sub>/PS-SiO<sub>2</sub> blends thin film annealed in acetone/heptane for 3 min. As is shown, a clear phase separation state was formed on the surface of PGNPs blends thin film. Then we put this film back to a neutral solvent for 3min, a homogeneous state on the surface was formed. Four cycles for the same film are conducted in our experiment. From d) to e), a homogeneous structure was successful back to phase separation state, which means this brush system can be reversible. Because of four cycles have been successfully reversed, we indicate that this system has a stable highly phase reversibility between two phase and one phase.

Since AFM is only a surface characterization technique and it cannot provide the morphologies underneath the top surface. We also used time of flight secondary ion mass spectroscopy (ToF-SIMS) analysis for this experiment. ToF-SIMS is a highly sensitive analytical technique that analyzes the chemical composition and distribution of a solid surface or thin film. It uses a range of incident ion sources to impact on solid surfaces and generate secondary ions that can be analyzed by a time of flight (or

Orbitrap) mass spectrometer to determine the surface chemistry of that surface or layer.

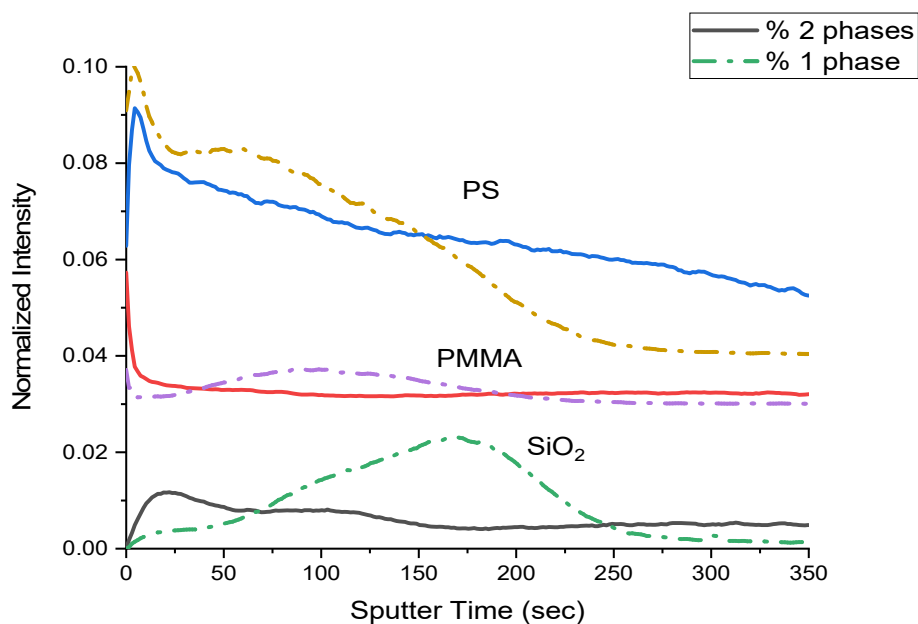


Figure 3.6. ToF-SIMS in-depth profile for PMMA-SiO<sub>2</sub>/PS-SiO<sub>2</sub> blends thin film at different phases

Figure 3.6 shows the in-depth mass spectroscopy of PGNP blends. The normalized intensity can stand for the composition of each component in PGNPs blends. As is shown, for one phase, the composition of PS decreased from the surface to the bottom, yet the composition of PMMA increased a little bit to a peak then decreased to a stable state from the surface to the bottom. This changing trend of each component clarifies that PS exists more on the surface and PMMA has more on the substrate. For the composition of SiO<sub>2</sub>, even though it has a similar changing trend with the composition of PMMA, it has more intensity peaks than PMMA. We believe this phenomenon is because of the actual nanostructure of PMMA-SiO<sub>2</sub>. Since the outer PMMA corona region needs to be sputtered away for the SiO<sub>2</sub> core can be detected. In the phase separation state, the composition of PS and PMMA decreased a little bit then become

stable. This illuminates that the composition of PS and PMMA will stay the same throughout the film.

As is indicated in chapter 1, the Flory-Huggins model can be used to investigate the phase behavior of PGNPs blends since the similar properties between PGNPs blends and polymer blends. Typically, the critical  $\chi N$  point for block copolymer is 10.5, but for polymer blends system is around 2. Therefore, the changing trend of the interaction parameter  $\chi$  and the degree of polymerization  $N$  is our research focus. In this experiment, the degree of polymerization is stable for PGNPs, so we assume that the interaction parameter would be changed with the difference of DIA solution composition. Based on Zeman's<sup>34</sup> study, he indicated that for polymer blends in a selective solution, when  $\chi_{\text{polymer1-solution}}$  is not equal to  $\chi_{\text{polymer2-solution}}$ , the  $\chi_{\text{polymer1-polymer2}}$  will increase. As expressed in equation 1.3, the relationship between the polymer-polymer interaction parameter and the difference between two polymer-solvent interaction parameters was developed by him,

$$\chi_{12} = \frac{(\chi_{1s} - \chi_{2s})^2}{(\delta_1 + \delta_2 - 2\delta_s)^2} \frac{RT}{v}, \quad \text{Equation 1.3}$$

he indicated that  $\chi_{12}$  is the key parameter that increased to induce the phase separation between polymer blends when this system is annealed in a selective solution. Compared to a selective solvent, a neutral solvent can induce a homogeneous state for polymer blends since it can decrease  $\chi_{12}$ . As we clarified in chapter 1, since the PGNPs blends has similar characters with polymer blends. We believed this theory can be applied to the PGNPs blends brush system when the degree of polymerization  $N$  is larger enough to drive the PGNPs blends brush system have a 'polymer-like' state.



Since the toluene is a good solvent for both PS and PMMA and toluene/heptane is a neutral solvent for PS/PMMA homopolymer blends system in DIA, we designed to add a different ratio of toluene to selective solvent acetone: heptane=1:2(volume ratio) to study the impact of the interaction parameter  $\chi$  on the phase behavior of PGNPs blends. Results are shown in figure 3.7 (i),

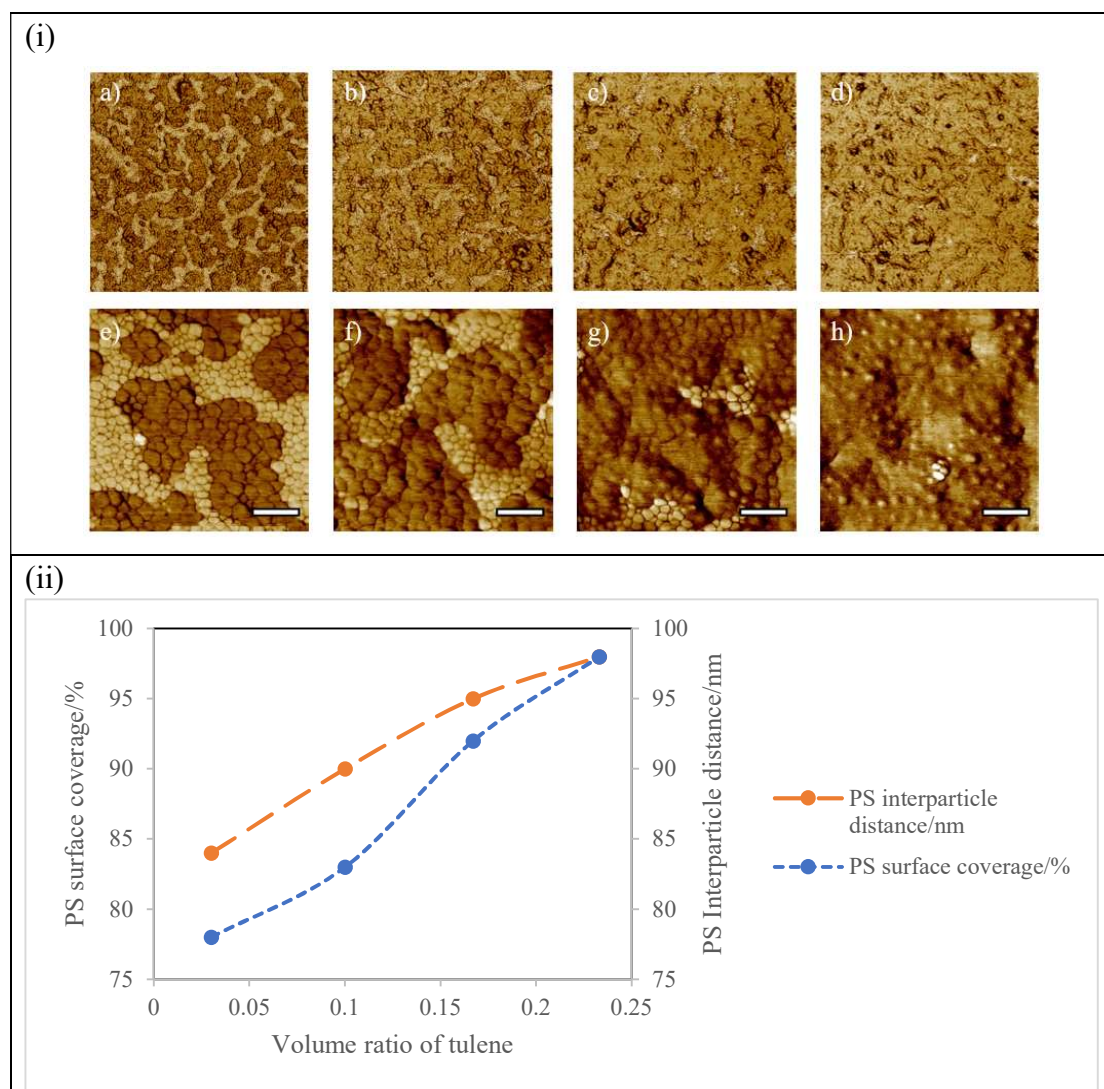


Figure 3.7 (i) AFM images as a function of volume ratio of toluene in fixed ratio acetone: heptane solution. (a) 3.3%; (b) 10.0%; (c) 16.7%; (d) 23.3% (Scale bar: 800 nm); (e)-(h) is the corresponded images in smaller scanning scale (Scale bar: 100nm) (ii). Calculated surface coverage and interparticle distances of PS-SiO<sub>2</sub> with different amount of toluene added.

the phase images of PGNPs blends thin films annealed in the selective solvent with different ratio of toluene for 1 minute. As is shown in figure 3.4, PGNPs blends thin film will present a phase separation state after annealed in a selective solvent-acetone/heptane. We believe the surface coverage and interparticle distance of PS can evaluate the impact of the interaction parameter  $\chi$ . We set four different ratios of toluene to the DIA solution: (a) 3.3%; (b) 10.0%; (c) 16.7%; (d) 23.3%. In figure 3.7 (i), a)- d) shows the dark area which stand for the PS phase coverage will increase with the toluene adding to the DIA solution. The changing trend of PS surface coverage is much more clear in detailed images shown as Figure 3.7.(i).e)-h). From the detailed images we can see that the phase separation state is apparent even for 16.7% toluene adding to the DIA selective solvent. Nonetheless, when we are making a comparison between e) and h), the boundary of the PS-SiO<sub>2</sub> become unclear. In image e), a whole PS-SiO<sub>2</sub> can still be observed, but in image h), the boundary between each PS-SiO<sub>2</sub> become disappeared. In image h), we can only see the inner core of PS-SiO<sub>2</sub>. The reason for this phenomenon is because of outer chains of PS-SiO<sub>2</sub> swelled since the impact of adding toluene to the selective solvent composition. This reason can be proved in figure 1.1, the brush region of a PGNP can be stretched or compressed. The self-boundary of PS-SiO<sub>2</sub> shown in figure 3.7 (i) e)-h) illuminate that with increasing the ratio of toluene added to the selective solvent, the extension of polymer chains will be broadened. The self-boundary changing trend of PS-SiO<sub>2</sub> is one way to track the impact of the interaction parameter  $\chi$  on the phase behavior of PGNPs blends.



The changing trend of the interparticle distance of PS-SiO<sub>2</sub> can also measure the impact of the interaction parameter  $\chi$ . In figure 3.7.(ii), it shows that the interparticle distance of PS-SiO<sub>2</sub> increases from 77.5 nm to 98.4 nm with adding toluene volume ratio from 3.3% to 23.3%. Our standpoint of a self-boundary changing trend with increasing the ratio of toluene added to the selective solvent, the extension of polymer chains will be broadened, can be also proved by this phenomenon. Another line shows the increasing trend of PS surface coverage. We believe the reason for the increasing trend of PS surface coverage is toluene could block the interaction of PS and PMMA, some small size PMMA-SiO<sub>2</sub> could be dissolved into PS-SiO<sub>2</sub> chains. This is also corresponding to the impact of the interaction parameter  $\chi$ .

### **3.2 Phase behavior of other PGNPs blends brush system**

As is stated in Chapter 1, PSAN-SiO<sub>2</sub> and PMMA-SiO<sub>2</sub> is an LCST system. Contrary to UCST systems, LCST blends are miscible at low temperatures, when the temperature is raised above the LCST, the blends will be phase separated. Compared to UCST polymer blends, LCST polymer blends have attracted much more attention as model systems in the study of polymer phase separation as this system can better control the phase separation process and the phase reversibly cycle between homogeneous state and phase separation state by subsequent heating and cooling.<sup>35</sup> For polymer grafted nanoparticle blends, the prospect of reversible phase separation is particularly interesting because it promises intriguing new opportunities to dynamically control the structure (and hence properties) of particle solids.<sup>13</sup>

In this chapter, we take a similar molecular characteristic of PSAN-SiO<sub>2</sub> and PMMA-SiO<sub>2</sub>. The molecular characteristics of these two particle brush system are summarized in Table 3.2.

Table 3.2 Summary of molecular characteristics of PSAN-SiO<sub>2</sub> and PMMA-SiO<sub>2</sub> particle brush system

Sample	N	Mn	Rc(nm)	$\sigma/\text{nm}^{-2}$
PSAN-SiO <sub>2</sub>	23600	150	35	0.68
PMMA-SiO <sub>2</sub>	23000	200	39	0.70

### 3.2.1 As cast study of LCST system PGNPs brush with ionic liquid

In this chapter, we analyzed the phase behavior of an LCST system: PSAN-SiO<sub>2</sub> and PMMA-SiO<sub>2</sub> to demonstrate the feasibility of phase reversibility of this PGNPs blends brush system. To accelerate the phase separation of this PGNPs blends, a small amount of ionic liquid (around 5%) is added to the PGNPs blends. We tried to use the thermal annealing to show the phase behavior because of DIA solution may wash the thin film out of the silicon wafer. Based on Huang and his coworker's research,<sup>36</sup> the glass transition temperature (T<sub>g</sub>) of PSAN-SiO<sub>2</sub> is around 105°C, and the LCST point of PSAN-SiO<sub>2</sub> and PMMA-SiO<sub>2</sub> is ranging from 155°C to 165°C, depending on the ratio of these two PGNPs. However, by adding ionic liquid to the PGNPs blends, the T<sub>g</sub> of PGNPs will decrease from 105°C to 95°C. In our experiment, we take a similar molecular characteristic of these two PGNPs and we assume that the LCST point for the PGNPs blends is 160°C. PGNPs blends thin film with thickness around 80 nm at 105°C (24hrs), 170°C (24 hours) was annealed. As cast state with different ratio of ionic liquid was shown below,

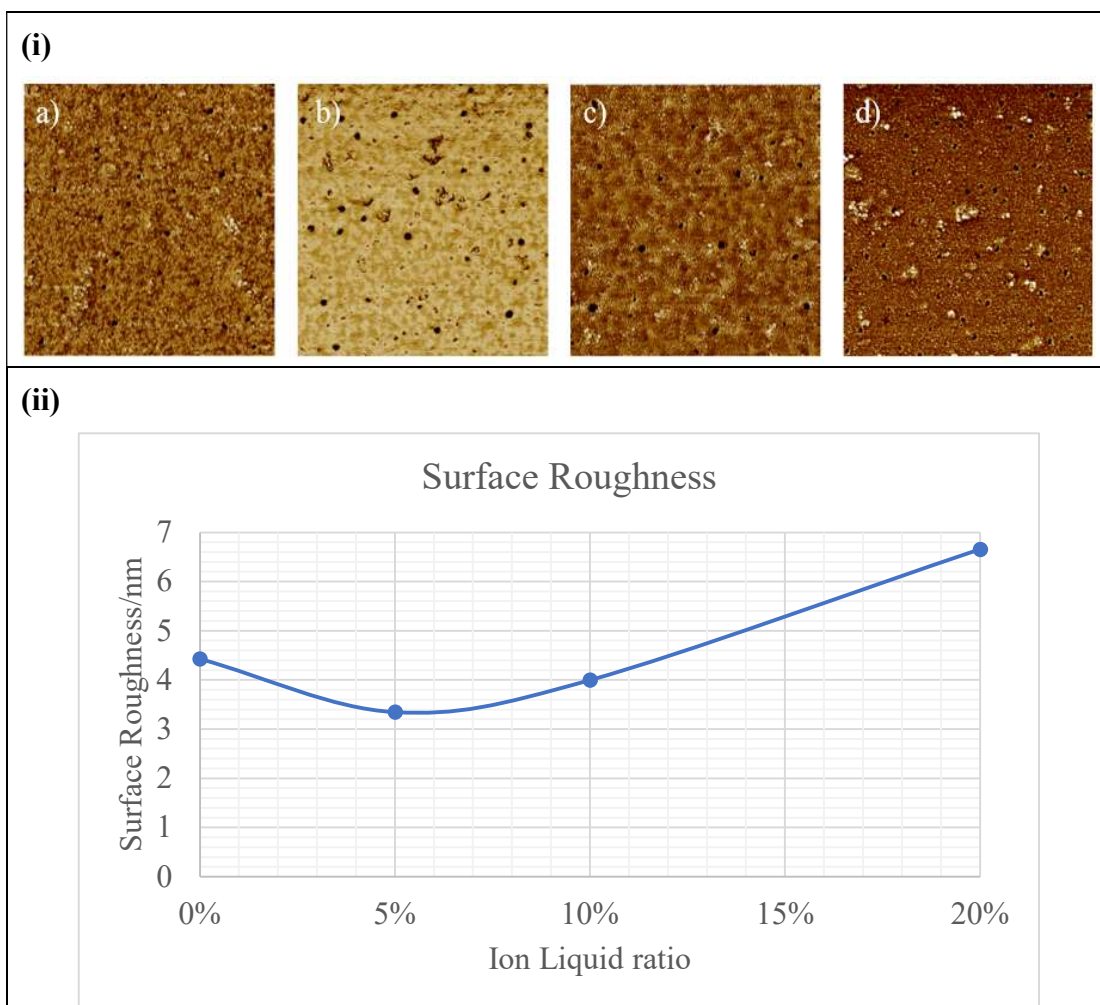


Figure 3.8 (i) AFM images of PGNPs blends thin film as cast state with different ratio of ionic liquid: a) 0%, b) 5%, c) 10%, d) 20% (Scale bar: 800nm); (ii) Surface roughness analysis of PGNPs blends thin film

in as cast state, PGNPs blends thin film exhibited a weakly phase-separated structure which is like UCST blends (not shown here). This can be rationalized by considering Hildebrand solubility parameters ( $\delta_{\text{PMMA}} = 19.0 \text{ MPa}^{\frac{1}{2}}$ ,  $\delta_{\text{PSAN}} = 19.6 \text{ MPa}^{\frac{1}{2}}$ ). Figure 3.8 (i) presents a phase behavior of PGNPs blends thin film. Yellow block is PSAN and dark block is PMMA. As is shown, with increasing the ratio of ionic liquid, the PMMA phase area gradually increased. We believe it is because of the impact of ionic liquid making PMMA chains swelled. Figure 3.8 (ii) shows the surface roughness changing

trend with increasing the ionic liquid ratio. The reason why surface roughness declined from 0% to 5% has been explained in the former chapter.

### 3.2.2 Phase reversibility of PSAN-SiO<sub>2</sub>/PMMA-SiO<sub>2</sub> system

Based on the as cast state film surface condition and phase behavior, we designed to measure the phase reversibility of PGNPs blends brush system with 5% ionic liquid. According to the polymer blends phase separation theory, upon the LCST point the PGNPs blends thin film should be homogeneous and below the LCST should be phase separated. However, the result we found become contradicted to the theory. Figure 3.9 shows the result,

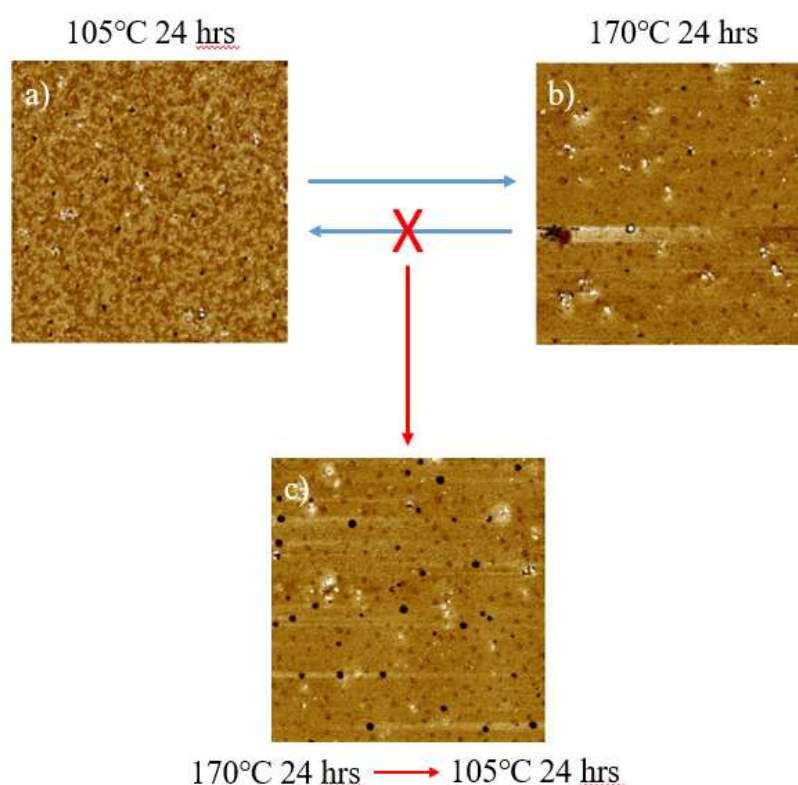


Figure 3.9 Schematic of phase reversibility test for 50PSAN-SiO<sub>2</sub>/50PMMA-SiO<sub>2</sub> blends (Scale bar: 800nm)

in figure 3.9 (a), we first put PGNPs blends thin film in 105°C-oven annealing for 24 hrs and it stays in phase separation state. Then we put this film into an oven with 170°C,

the phase state turns into the homogeneous state. We believe the reason for this phenomenon is because of the as cast state. This PGNPs blends thin film may dynamically track to the substrate when we are casting film. It will make the phase behavior of PGNPs blends thin film difficult since this behavior needs a lot of energy. We believe 105°C is not enough for the PGNPs to move in a thin film but 170°C is enough. However, things became more interesting when we put the same film back into the oven with 105°C, PGNPs blends thin film stays in the homogeneous state without turning back to phase separation state. This is contradicted with polymer blends phase reversibility theory. In order to make the phase reversibility of this LCST PGNPs blends brush system, we also tried three other possible solutions:

1. We cast thicker films and put them into an oven for longer time;
2. We elevated the oven's temperature from 170°C to 230°C;
3. We cast some films without adding ionic liquid, then repeat the thermal annealing procedure.

All results we collected from these three possible solutions stays the same-this system's phase behavior under AFM scanning is not reversible. We believe that there is one possible reason can explain this problem: thermal annealing will flatten the surface of PGNPs blends thin film and PMMA-SiO<sub>2</sub> will be covered by PSAN-SiO<sub>2</sub> after thermal annealing. We believe that for temperature upon 160°C, there is a great enthalpic force that squeezes the PMMA-SiO<sub>2</sub> to the bottom and makes PSAN-SiO<sub>2</sub> elevated up to the surface. This phenomenon may form a layered structure. Therefore,

we verified it by using tof-sims test to show the composition underneath the surface of PGNPs blends thin film. Figure 3.10 shows the result,

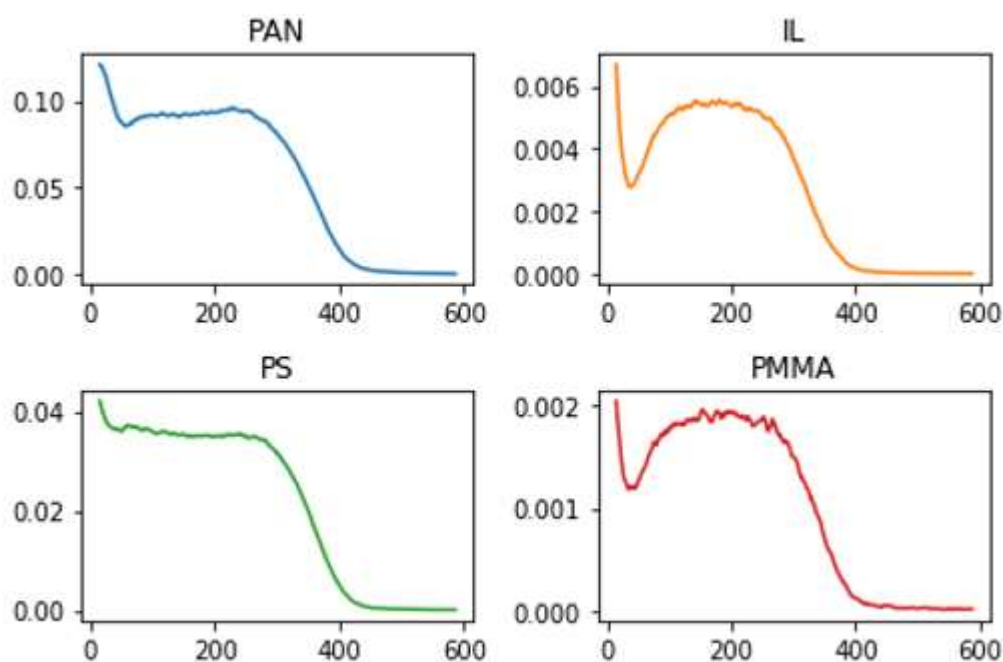


Figure 3.10 ToF-SIMS in-depth profile for PMMA-SiO<sub>2</sub>/PSAN-SiO<sub>2</sub> blends thin film at different phases annealed at 170°C for 24 hrs

the composition of PSAN is decreased a little bit then stays in a stable intensity and finally goes down to the bottom. Compared with the changing trend of PSAN, the composition of PMMA has a similar changing trend with ionic liquid. In figure 3.10, both the composition of PMMA and ionic liquid decreased to a bottom from the surface, then increased to a stable state, and finally decreased to zero. After 160s, the composition and changing trend of PMMA and PSAN will stay the same. This illuminates that the composition of PSAN-SiO<sub>2</sub> and PMMA-SiO<sub>2</sub> will stay the same below a certain depth of the thin film and these two PGNPs should be phase separated. This is corresponding to what we speculate before. After this PGNPs blends thin film annealed in 170°C for 24 hrs, it will be phase separated underneath the thin film surface

and form a layer structure, which cannot be detected from an AFM phase image. Future research can focus on the layer structure of this PGNPs blends brush system, we will not address it more here.

## 4. Conclusion

In this thesis, we investigate the phase behavior of two different PGNPs blends system under DIA and thermal annealing condition: PS-SiO<sub>2</sub>/PMMA-SiO<sub>2</sub>(UCST system) and PSAN-SiO<sub>2</sub>/PMMA-SiO<sub>2</sub>(LCST system). We also investigate the impact of a small amount of ionic liquid on the phase separation of PGNPs blends thin film. Here are the conclusions.

1%, 5%, 10%, 25% ionic liquid were chosen for PS-SiO<sub>2</sub>/PMMA-SiO<sub>2</sub> blends. From our experiment results, ionic liquid will accelerate the process of phase separation and make the thin film surface become roughness. Adding ionic liquid to the PGNPs blends will increase the interaction parameter  $\chi$ . We also did a time dependent study of PGNPs blends thin film with different ratio of ionic liquid. Even though a small amount of ionic liquid could accelerate the speed of phase separation, it will also make a significant height difference in the thin film state which is not desired for our phase reversibility experiment.

A successful phase reversibility result of PS-SiO<sub>2</sub>/PMMA-SiO<sub>2</sub> blends thin film was shown in chapter 3. We proved that PS-SiO<sub>2</sub>/PMMA-SiO<sub>2</sub> blends brush system will have a ‘polymer blends like’ phase behavior which is known as UCST. From our results, we demonstrated the key reason for the phase reversibility of PS-SiO<sub>2</sub>/PMMA-SiO<sub>2</sub> is the difference of interaction parameter  $\chi_{\text{PMMA-PS}}$ . A selective DIA solvent can increase the interaction parameter and induce phase separation, while a neutral DIA solvent can decrease the interaction parameter and induce homogeneous phase state. We also clarified that polymer chains grafted on the nanocore could be swelled if the



PGNPs blends thin film are annealed in a good solvent. The ability of a nanoscale phase reversibility could enable transformative advances in the high-throughput fabrication of solid films with tailored and mutable structures and properties that play an important role in a range of nanoparticle-based polymer material technologies.

We also investigated the phase behavior of the PSAN-SiO<sub>2</sub>/PMMA-SiO<sub>2</sub> blends with or without ionic liquid. The result is the same as PS-SiO<sub>2</sub>/PMMA-SiO<sub>2</sub> blends brush system when adding ionic liquid to the blends. PMMA covered the surface gradually with the increase of ionic liquid ratio. But for phase reversibility results of PSAN-SiO<sub>2</sub>/PMMA-SiO<sub>2</sub> blends thin film with adding 5% ionic liquid. This system's phase behavior is not coordinated with the UCST system. We suspect there is layer structure formed in this PGNPs blends thin film. From the result of ToF-SIMS test, the composition of PSAN-SiO<sub>2</sub> and PMMA-SiO<sub>2</sub> will stay the same below a certain depth of the thin film after annealed in 170°C for 24 hrs. A layer structure of PSAN-SiO<sub>2</sub>/PMMA-SiO<sub>2</sub> was formed underneath the surface of thin film. A layer structure should be the future research orientation.

## References:

1. Striemer, C. C.; Krishnan, R. & Fauchet, P. M. "The development of nanocrystalline silicon for emerging microelectronic and nanoelectronic applications." *Jom* 56, 20–25 (2004).
2. Odom, T. W.; Pileni, M.P. "Nanoscience." *Acc. Chem. Res* 41, 1565 (2008).
3. Talapin, D. V.; Lee, J. S.; Kovalenko, M. V.; Shevchenko, E. V. "Prospects of colloidal nanocrystals for electronic and optoelectronic applications." *Chem. Rev.* 110, 389–458 (2010).
4. Balazs, A. C.; Emrick, T.; Russell, T. P. "Nanoparticle Polymer Composites: Where Two Small Worlds Meet." *Science* 314 (5802), 1107–1110 (2006).
5. Hui, C M.; Pietrasik, J.; Schmitt, M.; Mahoney, C.; Choi, J.; Bockstaller M.; Matyjaszewski K. "Surface-initiated polymerization as an enabling tool for multifunctional (nano-) engineered hybrid materials." *Chem. Mater.* 26, 745–762 (2014).
6. Panayiotis, V.; Jihoon, C.; Hongchen, D.; Michael, R. B.; Krzysztof, M.; George, F. "Interaction between polymer-grafted nanoparticles." *Macromolecules* 42 (7), 2721–2728 (2009).
7. Mackay, M. E.; Tuteja, A.; Duxbury, P. M.; Hawker, C. J.; Van Horn, B.; Guan, Z.; Chen, G.; Krishnan, R. S. "General Strategies for Nanoparticle Dispersion." *Science* 311 (5768), 1740–1743 (2006).
8. *Dekker Encyclopedia of Nanoscience and Nanotechnology*. (2007).

9. Tambasco, M., Lipson, J. E. G., Higgins, J. S. "Blend Miscibility and the Flory–Huggins Interaction Parameter: A Critical Examination." *Macromolecules* 39 (14), 4860–4868 (2006).
10. Modi, A.; Bhaway, S M.; Vogt, B D.; Douglas, J F.; Al-Enizi, A.; Elzatahry, A.; Sharma, A.; Alamgir, K. "Direct Immersion Annealing of Thin Block Copolymer Films." *ACS Applied Materials & Interfaces* 7 (39), 21639-21645 (2015).
11. Verma, A.; Sharma, A. "Enhanced Self-Organized Dewetting of Ultrathin Polymer Films under Water-Organic Solutions: Fabrication of Sub-Micrometer Spherical Lens Arrays." *Adv. Mater.* 22, 5306–5309 (2010).
12. Park, W. I.; Kim, J. M.; Jeong, J. W. & Jung, Y. S. "Deep-nanoscale pattern engineering by immersion-induced self-assembly." *ACS Nano* 8, 10009–10018 (2014).
13. Schmitt, M.; Zhang J.; Lee J., Bongjoo L.; Xin N.; Ren Z.; Karim A.; Robert F. Davis.; Krzysztof M.; Micheal R. B. "Polymer ligand–induced autonomous sorting and reversible phase separation in binary particle blends." *Sci. Adv.* 2, e1601484 (2016).
14. Choi, J.; Chin, M. H.; Joanna, P.; Hongchen, D.; Krzysztof, M.; Micheal, R. B. "Toughening fragile matter: Mechanical properties of particle solids assembled from polymer-grafted hybrid particles synthesized by ATRP." *Soft Matter* 8, 4072–4082 (2012).

15. Choi, J.; Dong, H.; Matyjaszewski, K.; Michael, R. B. "Flexible particle array structures by controlling polymer graft architecture." *J. Am. Chem. Soc.* **132**, 12537–12539 (2010).
16. Kumar, S. K.; Jouault, N.; Benicewicz, B. & Neely, T. "Nanocomposites with polymer grafted nanoparticles." *Macromolecules* **46**, 3199–3214 (2013).
17. Akcora, P., Liu, H., Kumar, S., Joseph, M., Yu, L., Brian, C. Benicewicz., Linda, S. S., Devrim, A., Athanassios, Z. P., Victor, P., Venkat, G., Jan, I., Pappanan, T., Ralph, H C. & Jack, F. D. "Anisotropic self-assembly of spherical polymer-grafted nanoparticles." *Nature Mater.* **8**, 354–359 (2009).
18. Xiaoteng, W.; Sonal, B.; Ren, Z., Praveen, P.; Dharmaraj, R.; Jianan, Z.; Michael, R. B.; Jack, F. D.; Alamgir, K. "Nanoimprinting Directed Assembly of Associating Polymer-Grafted Nanoparticles for Polymer Thin Films with Enhanced Stability." *ACS Appl. Polym. Mater.* (2019).
19. Xuanxuan, C.; Chun, Z.; Shuang-Jun, C.; Gordon, S. W. Craig.; Paulina, R. D.; Takahiro, D.; Ken, M.; Takaya, M.; Akiyoshi, Y.; Roel, G.; Mark, P. S.; Paul, F. N. "Ionic Liquids as Additives to Polystyrene-Block-Poly(Methyl Methacrylate) Enabling Directed Self-Assembly of Patterns with Sub-10 nm Features." *ACS Applied Materials & Interfaces* **10** (19), 16747-16759 (2018).
20. Longanecker, M. Arvind, M., Andrey, D., Seyong, K., Guangcui, Y., Ronald, J., Sushil, S., Joona, B., Alamgir, K. "Reduced domain size and interfacial width in fast ordering nanofilled block copolymer films by direct immersion annealing." *Macromolecules* **49**, 8563–8571 (2016).

21. Harton, S. E.; Kumar, S. K. “Mean-Field Theoretical Analysis of Brush-Coated Nanoparticle Dispersion in Polymer Matrices.” *Journal of Polymer Science Part B Polymer Physics* 46, 351–358 (2008).
22. Park, W. I.; Kim, J. M.; Jeong, J. W. & Jung, Y. S. “Deep-nanoscale pattern engineering by immersion-induced self-assembly.” *ACS Nano* 8, 10009–10018 (2014).
23. Noboru, H.; Jörg, K.; Takashi, Inoue. “Lower critical solution temperature and upper critical solution temperature phase behaviour in random copolymer blends: poly(styrene-co-acrylonitrile)/poly(methyl methacrylate) and poly(styrene-co-acrylonitrile)/poly( $\epsilon$ -caprolactone).” *Polymer* 36(14), 2761-2764 (1995).
24. Paul, D. R.; Barlow, J. W. “A binary interaction model for miscibility of copolymers in blends.” *Polymer* 25, 487–494 (1984)
25. Wen, G.; Sun Z.; Shi T.; Yang J.; Jiang W.; An L.; Li, B. “Thermodynamics of PMMA/SAN: Application of the Sanchez – Lacombe lattice fluid theory.” *Macromolecules* 34, 6291–6296 (2001).
26. Matyjaszewski, K.; Tsarevsky, N. V. “Nanostructured functional materials prepared by atom transfer radical polymerization.” *Nature Chem.* 1, 276–288 (2009).
27. Chung, H. j.; Composto, R. J. “Breakdown of dynamic scaling in thin film binary liquids undergoing phase separation.” *Phys. Rev. Lett.* 92, 185704 (2004).
28. Russell, T. P.; Hjelm, Jr.R. P.; Seeger, P. A. “Temperature dependence of the interaction parameter of polystyrene and poly(methyl methacrylate).” *Macromolecules* 23, 890–893 (1990).

29. Simone, P. M.; Lodge, T. P. "Lyotropic Phase Behavior of Polybutadiene-Poly(ethylene Oxide) Diblock Copolymers in Ionic Liquids." *Macromolecules* 41, 1753–1759 (2008).
30. Virgili, J. M.; Hexemer, A.; Pople, J. A.; Balsara, N. P.; Segalman, R. A. "Phase Behavior of Polystyrene-Block-poly(2-Vinylpyridine) Copolymers in a Selective Ionic Liquid Solvent." *Macromolecules* 42, 4604–4613 (2009).
31. Miranda, D. F.; Russell, T. P.; Watkins, J. J. "Ordering in Mixtures of a Triblock Copolymer with a Room Temperature Ionic Liquid." *Macromolecules* 43, 10528–10535 (2010).
32. Li, W.; Nealey, P. F.; de Pablo, J. J.; Muller, M. "Defect Removal in the Course of Directed Self-Assembly Is Facilitated in the Vicinity of the Order-Disorder Transition." *Phys. Rev. Lett.* 113, 168301. (2014).
33. Koenig, J. L. "Dissolution of Symmetric Diblock Copolymers with Neutral Solvents, a Selective Solvent, a Nonsolvent, and Mixtures of a Solvent and Nonsolvent Monitored by FT-IR Imaging." *Macromolecules* 36, 4851–4861 (2003).
34. Zeman, L. & Patterson, D. "Effect of the Solvent on Polymer Incompatibility in Solution." *Macromolecules* 5, 513–516 (1972).
35. Lin, C. C.; Jeon, H. S.; Balsara, N. P.; Hammouda B. "Spinodal decomposition in multicomponent polymer blends." *J. Chem. Phys.* 103, 1957–1971 (1995).
36. Huang, C.; Gao, J.; Yu, W.; Zhou, C. "Phase Separation of Poly(methyl methacrylate)/Poly(styrene-co-acrylonitrile) Blends with Controlled Distribution of Silica Nanoparticles." *Macromolecules* 45 (20), 8420-8429 (2012).